New Journal of Physics
The open access journal at the forefront of physics

Deutsche Physikalische Gesellschaft DPG
IOP Institute of Physics

Published in partnership with: Deutsche Physikalische Gesellschaft and the Institute of Physics

OPEN ACCESS

RECEIVED
14 November 2020

REVISED
2 May 2021

ACCEPTED FOR PUBLICATION
10 May 2021

PUBLISHED
11 June 2021

PAPER

Supersymmetry with self-consistent Schrödinger–Poisson equations: finding partner potentials and breaking symmetry

Amine Abouzaid* and **A F J Levi**

Department of Electrical and Computer Engineering, University of Southern California, Los Angeles, CA 90089-2533, United States of America

* Author to whom any correspondence should be addressed.

E-mail: abouzaid@usc.edu

Keywords: supersymmetric quantum mechanics, supersymmetry, self-consistent Schrödinger equation, Schrödinger–Poisson equation

Abstract

It is shown that isospectral Hamiltonians and partner potentials can be found for self-consistent solutions of the Schrödinger and Poisson equations in the presence of identical non-interacting electrons. Perturbation of these systems by an external electric field can be used to break symmetry and spectrally distinguish between states. For a given pair of partner potentials, symmetry may also be broken by a change of electron density or temperature.

1. Introduction

Supersymmetric quantum mechanics describes Hamiltonians with time-independent potentials whose partner Hamiltonians are isospectral (with the possible exception of the ground state), but do not necessarily have the same eigenfunctions [1–3]. It is also possible, using supersymmetric quantum mechanics, to describe families of Hamiltonians with strictly isospectral eigenvalues [3–5]. Therefore, supersymmetry may be considered a *resource* to create spectrally identical systems with different eigenstates. Recent applications of supersymmetric quantum mechanics include spectral design of electron states in Schrödinger Hamiltonian systems [6], analytic solutions for electrons in graphene [7], and the design of laser arrays [8, 9].

The existence of isospectral Hamiltonians and their associated partner potentials leaves unanswered how they may be distinguished. Such questions are analogous to the well-known problem of 'hearing the shape of a drum' [10]. In the case of partner potentials, the isospectral nature of the corresponding Hamiltonians precludes the possibility of 'hearing' any difference between the unaltered potentials. However, it is possible to separate the eigenvalues of the partner potentials by introducing perturbations, thereby exploiting the fact that the eigenfunctions (and the perturbed potentials themselves) are not identical. In particular, a uniform electric field can often be used to separate the energy eigenvalues of a single-electron Hamiltonian and its supersymmetric partner. For certain potentials, these changes in energy eigenvalues can provide a sensitive method of distinguishing otherwise isospectral systems (see subsection 7.2).

In a condensed matter system such as a doped semiconductor, the presence of an ionized-charge donor concentration and band-edge potential profile requires a self-consistent solution of the Schrödinger and Poisson equations. Prior research on supersymmetry in semiconductor systems has not addressed this self-consistency [11,12]. In the following, we study this for the special case of non-interacting electrons in a semiconductor quantum well structure. The Schrödinger and Poisson equations are solved simultaneously to account for the effect of the charge distribution on the potential [13–16], as described in section 3.

Generally, it is not obvious that supersymmetry can be applied to systems that include the presence of many electrons. The earliest formulations of supersymmetric quantum mechanics relate to the Schrödinger equation describing the wavefunction of a single particle. Such a formulation is not sufficient in the presence of ionized donors, as discussed in section 6. Evaluating partner potentials in the presence of multiple non-interacting charged particles described by coupled Schrödinger and Poisson equations

requires a modified method, as described in section 5. This latter method is used to explore symmetry breaking in sections 7 and 8.

2. Supersymmetric quantum mechanics

A single electron of bare mass m_0 in a (non-self-consistent) potential well $V(x)$ has a ground state ψ_0 with eigenenergy E_0. If $V^{(-)}(x) = V(x) - E_0$, the Hamiltonian

$$\hat{H}^{(-)} = -\frac{\hbar^2}{2m_0}\frac{\mathrm{d}^2}{\mathrm{d}x^2} + V^{(-)}(x) \tag{1}$$

has ground state ψ_0 with eigenenergy $E_0^{(-)} = 0$, from which it follows that

$$\hat{H}^{(-)}\psi_0(x) = -\frac{\hbar^2}{2m_0}\frac{\mathrm{d}^2\psi_0}{\mathrm{d}x^2} + V^{(-)}(x)\psi_0 = 0 \tag{2}$$

so that (adopting the notation $\psi_0'' = \frac{\mathrm{d}^2\psi_0}{\mathrm{d}x^2}$)

$$V^{(-)}(x) = \frac{\hbar^2}{2m_0}\frac{\psi_0''}{\psi_0}. \tag{3}$$

If $\hat{A} = \frac{\hbar}{\sqrt{2m_0}}\frac{\mathrm{d}}{\mathrm{d}x} + W(x)$, where the superpotential $W(x) = -\frac{\hbar}{\sqrt{2m_0}}\frac{\psi_0'}{\psi_0}$, then $\hat{H}^{(-)} = \hat{A}^\dagger\hat{A}$ [3]. The Hamiltonian

$$\hat{H}^{(+)} = \hat{A}\hat{A}^\dagger = -\frac{\hbar^2}{2m_0}\frac{\mathrm{d}^2}{\mathrm{d}x^2} + V^{(+)}(x) \tag{4}$$

is then the supersymmetric partner of $\hat{H}^{(-)}$, where [17, 18]

$$V^{(+)}(x) = -V^{(-)}(x) + \frac{\hbar^2}{m_0}\left[\frac{\psi_0'}{\psi_0}\right]^2. \tag{5}$$

If $\psi_n^{(-)}$ is an eigenfunction of $\hat{H}^{(-)}$ with eigenenergy $E_n^{(-)}$, then

$$\begin{aligned}\hat{H}^{(+)}\left(\hat{A}\psi_n^{(-)}\right) &= \hat{A}\hat{A}^\dagger\hat{A}\psi_n^{(-)} \\ &= \hat{A}\hat{H}^{(-)}\psi_n^{(-)} = E_n^{(-)}\left(\hat{A}\psi_n^{(-)}\right).\end{aligned} \tag{6}$$

Thus $\hat{A}\psi_n^{(-)}$ is an eigenfunction of $\hat{H}^{(+)}$ with eigenenergy $E_n^{(+)} = E_n^{(-)}$. If $\psi_n^{(-)}$ is normalized, so that $\langle\psi_n^{(-)}|\psi_n^{(-)}\rangle = 1$, then

$$\begin{aligned}\langle\hat{A}\psi_n^{(-)}|\hat{A}\psi_n^{(-)}\rangle &= \langle\psi_n^{(-)}|\hat{A}^\dagger\hat{A}|\psi_n^{(-)}\rangle \\ &= \langle\psi_n^{(-)}|\hat{H}|\psi_n^{(-)}\rangle = E_n^{(-)}.\end{aligned} \tag{7}$$

Therefore, the normalized eigenfunctions of $V^{(+)}(x)$ are [17, 18]

$$\psi_n^{(+)} = \frac{1}{\sqrt{E_n^{(-)}}}\hat{A}\psi_n^{(-)}, \tag{8}$$

where $n = 1, 2, 3, \ldots$. The $\psi_n^{(+)}$ states are numbered starting from 1 because there is no $\psi_n^{(+)}$ state with the same energy as the $\psi_0^{(-)}$ state.

3. Self-consistent model

The model we adopt requires self-consistency between solutions to the Schrödinger equation for non-interacting electrons and the Poisson equation describing the total static potential due to the spatially varying charge distribution [13–16]. The many-body Coulomb interaction between electrons is ignored.

3.1. Zero temperature

Consider a semiconductor medium of permittivity ϵ that is configured as a planar potential well with on-site potential $V_{\mathrm{os}}(x)$. An ionized donor concentration $N_{\mathrm{D}}(x)$ creates a density $n(x)$ of electrons in the conduction band. Effective electron mass is m_{e}^* and the electrons are assumed to be non-interacting. Each electron is constrained to motion in the x-direction and each state obeys the Schrödinger equation

$$-\frac{\hbar^2}{2m_{\mathrm{e}}^*}\frac{\mathrm{d}^2}{\mathrm{d}x^2}\psi(x) + V_{\mathrm{tot}}(x)\psi(x) = E\psi(x), \tag{9}$$

where

$$V_{\text{tot}}(x) = V_{\text{c}}(x) + V_{\text{os}}(x) \tag{10}$$

and the electric potential energy due to ionized donors and other electrons in the conduction band is $V_{\text{c}} = -e\Phi(x)$ [13]. The electric potential $\Phi(x)$ satisfies Poisson's equation

$$\frac{\text{d}}{\text{d}x}\left(\epsilon\frac{\text{d}}{\text{d}x}\right)\Phi(x) = -e(N_{\text{D}}(x) - n(x)), \tag{11}$$

where $n(x)$ is the electron density

$$n(x) = \sum_j n_j|\psi_j(x)|^2, \tag{12}$$

and n_j is the two-dimensional density of the jth electron sub-band state.

Since the system is charge-neutral, the integrated electron density equals the integrated ionized donor concentration, so that

$$\begin{aligned}\int N_{\text{D}}(x)\text{d}x &= \int n(x)\text{d}x \\ &= \int \sum_j n_j|\psi_j(x)|^2\text{d}x = \sum_j n_j.\end{aligned} \tag{13}$$

Furthermore, if the system is assumed to be at zero absolute temperature, then electrons will occupy states up to the Fermi energy E_{F}, so that

$$n_j = (E_{\text{F}} - E_j)D, \tag{14}$$

for eigenvalues $E_j < E_{\text{F}}$, where $D = \frac{m_e^*}{\pi\hbar^2}$ is the density of states of a two-dimensional sub-band, accounting for spin. It follows that

$$E_{\text{F}} = \frac{\int N_{\text{D}}(x)\text{d}x - \sum_{j=1}^{N_{\text{F}}} E_j D}{N_{\text{F}}D}. \tag{15}$$

The only remaining unknown is N_{F}, the index of the highest occupied eigenstate which may be found iteratively.

Note that in order to determine $n(x)$, an approximation of the eigenstates ψ_j and eigenvalues E_j of equation (9) must already be known. Thus, in the first iteration, equation (9) can be solved by substituting $V_{\text{tot}}(x) = V_{\text{os}}$ to find the first approximation of the eigenstates and eigenvalues.

Once $n(x)$ has been determined, equation (11) can be solved, and the value of $\Phi(x)$ can be substituted into equation (10) to find the next approximation of V_{tot}, which is then substituted into equation (9) to find new approximations of ψ_j and E_j. A new electron density $n(x)$ can then be evaluated and substituted back into equation (11), and the process is repeated until convergence to within a specified relative error is reached. To ensure convergence, at the nth iteration, the new total potential $V_{\text{tot}}(n; x)$ is taken to be a linear combination of the potential calculated by the above procedure $V_{\text{tot}}(x)$ and the total potential from the prior iteration $V_{\text{tot}}(n-1; x)$, so that $V_{\text{tot}}(n; x) = \alpha V_{\text{tot}}(x) + (1-\alpha)V_{\text{tot}}(n-1; x)$, where the relaxation constant α has a value between 0 and 1 [15].

3.2. Finite temperature

At finite absolute temperature T, the two-dimensional density of the jth electron sub-band state is

$$n_j = \int_{E_j}^{\infty} Df(E)\text{d}E, \tag{16}$$

where $f(E) = \frac{1}{\text{e}^{(E-\mu)/k_{\text{B}}T}+1}$ is the Fermi–Dirac distribution describing occupation of n electron states in thermal equilibrium.

The chemical potential μ must be determined to evaluate n_j. Note that while D is the density of states for a single sub-band, the presence of multiple sub-bands means that the total density of states accounting for all sub-bands is

$$D^*(E) = \sum_j D\Theta(E - E_j), \tag{17}$$

where $\Theta(E)$ is the unit step function, and E_j is the lowest eigenenergy of the jth sub-band.

From this, it follows that the total two-dimensional electron density is

$$n_{2\text{D}} = \int n(x)\text{d}x = \int D^*(E)f(E)\text{d}E, \tag{18}$$

recalling that, due to charge neutrality of the medium, $n_{2D} = \int n(x)\mathrm{d}x = \int N_D(x)\mathrm{d}x$, where $N_D(x)$ is the ionized donor density. The only unknown in equation (18) is the chemical potential μ.

Iteration is used to solve for μ. The upper bound for μ is set to $\mu_{max} = n_{2D}\frac{\pi\hbar^2}{m_e^*}$, where μ_{max} is what the Fermi energy would be if only a single sub-band were occupied. For numerical calculations, the lower bound is set to $\mu_{min} = -k_B T \ln\left(N_{max}\ k_B T/E_F\right)$, where N_{max} is the index of the highest energy eigenstate included in the calculation. The index N_{max} should be greater than the index of the highest energy eigenstate that is not negligibly occupied.

An initial value $\mu' = (\mu_{min} + \mu_{max})/2$ is used. If $n_{2D} \leqslant \int D*(E)f(E)\mathrm{d}E$, then $\mu' \geqslant \mu$, and the upper bound is then updated to $\mu_{max} = \mu'$. Otherwise, $\mu' < \mu$, and the lower bound is updated to $\mu_{min} = \mu'$. Another iteration can then be made with an updated value of $\mu' = (\mu_{min} + \mu_{max})/2$, and this continues until $n_{2D} = \int D*(E)f(E)\mathrm{d}E$ to within a desired relative error.

The value of μ calculated this way may then be used to calculate the two-dimensional densities n_j using equation (16), from which the electron density $n(x)$ is then evaluated using equation (12). Once the electron density $n(x)$ has been determined, the calculation proceeds in the same manner as in the zero temperature case to find new approximations of the total potential V_{tot}, the eigenfunctions ψ_j and the eigenenergies E_j. The chemical potential μ must then be reevaluated, and this process is repeated until convergence to within a specified relative error is reached.

4. On-site potentials that yield target total potentials

Given a system with non-interacting electrons of effective mass m_e^*, ionized donor density $N_D(x)$, temperature T, and a target total potential $V_{target}(x)$, it is possible to determine an on-site potential $V_{os}(x)$ that yields, upon solution of the Shrödinger–Poisson equations, a total potential $V_{tot}(x) = V_{target}(x)$.

If a total potential $V_{tot}(x) = V_{target}(x)$ is postulated, then the eigenstates $\psi_j(x)$ and eigenenergies E_j can be determined by solving the Schrödinger equation

$$-\frac{\hbar^2}{2m_e^*}\frac{\mathrm{d}^2}{\mathrm{d}x^2}\psi_j(x) + V_{target}(x)\psi_j(x) = E_j\psi_j(x) \tag{19}$$

without iterating for self-consistency. The chemical potential μ can then be found based on the ionized donor density $N_D(x)$, the temperature T and the eigenenergies E_j, as described in subsection 3.2. The two-dimensional density n_j of the electron sub-band states can then be evaluated using equation (16). The total electron density $n(x)$ is then determined by equation (12), and the Poisson equation (equation (11)) is solved to find the electric potential $\Phi(x)$ due to the ionized donors and conduction band electrons. It follows from equation (10) that the on-site potential is

$$V_{os}(x) = V_{target}(x) + e\Phi(x). \tag{20}$$

This on-site potential, when substituted into the Schrödinger–Poisson equations and solved self-consistently as described in section 3, will yield the desired total potential $V_{tot}(x) = V_{target}(x)$ and eigenstates $\psi_j(x)$ with eigenenergies E_j.

To see that this must be the case, suppose that the eigenstates $\psi_j(x)$ and eigenenergies E_j of the target total potential $V_{target}(x)$ are used as the initial condition to solve the Schrödinger–Poisson equations, together with the on-site potential $V_{os}(x) = V_{target}(x) + e\Phi(x)$. Then, following the process described above, the same chemical potential μ, and thus the same electric potential $\Phi(x)$ will be found at the first iteration, so that the total potential, according to equation (10), is

$$V_{tot}(x) = -e\Phi + V_{os}(x) = V_{target}(x). \tag{21}$$

The total potential would thus converge to the desired potential at the first iteration.

In practice, it is not necessary to use $\psi_j(x)$ and E_j as the initial conditions. The process described in section 3 can be used unaltered once $V_{os}(x)$ has been evaluated, and the total potential $V_{tot}(x)$ will asymptotically converge to the desired potential $V_{target}(x)$ as the number of iterations increases (as has been verified numerically).

5. Supersymmetry with self-consistent Schrödinger–Poisson equations

It may seem that supersymmetry is incompatible with self-consistent solutions of the Schrödinger equation, due to the fact that the eigenstates and eigenenergies of a system with given on-site potential $V_{os}(x)$ and nonzero ionized donor density $N_D(x)$ solved using the Schrödinger–Poisson equations will differ from the

eigenstates and eigenenergies that would be found for a system with the same on-site potential $V_{os}(x)$ solved using the *non*-self-consistent Schrödinger equation. Thus, if partner on-site potentials $V_{os}^{(+)}(x)$ and $V_{os}^{(-)}(x)$ were to be evaluated using the method described in section 2 without accounting for self-consistency, the eigenvalues $E_n^{(+)}$ and $E_n^{(-)}$ found upon substituting those on-site potentials into the Schrödinger-Poisson equations with nonzero ionized donor density $N_D(x)$ would not be equal (i.e. the systems would not be isospectral).

However, supersymmetry and the Schrödinger-Poisson equations can be reconciled by noting that it is the final total potential $V_{tot}(x)$, found upon convergence of the solutions of the Schrödinger-Poisson equations, that determines the eigenstates and eigenenergies of the system. Once this total potential is known, it can be substituted into the Schrödinger equation, and the partner total potentials $V_{tot}^{(+)}(x)$ and $V_{tot}^{(-)}(x)$ can be found by using the method described in section 2. It then remains to find the on-site potentials $V_{os}^{(+)}(x)$ and $V_{os}^{(-)}(x)$ that generate these supersymmetric partner total potentials, using the method described in section 4.

Given a semiconductor medium with on-site potential $V_{os}(x)$, ionized donor density $N_D(x)$, temperature T, permittivity ϵ, and effective electron mass m_e^*, let ψ_n and E_n be solutions of the self-consistent Schrödinger-Poisson equations (equation (9)), and let $V_{tot}(x) = V_c + V_{os}$ be the total potential experienced by these solutions, where $V_c = -e\Phi$. Since $V_{tot}(x)$ is the final total potential, it can be used to calculate supersymmetric partner total potentials $V_{tot}^{(+)}(x)$ and $V_{tot}^{(-)}(x)$, with eigenfunctions and eigenvalues $\psi_n^{(+)}$, $E_n^{(+)}$, $\psi_n^{(-)}$, and $E_n^{(-)}$, using the method shown in section 2. These total potentials are isospectral.

To find the on-site potentials $V_{os}^{(+)}(x)$ and $V_{os}^{(-)}(x)$ that generate $V_{tot}^{(+)}(x)$ and $V_{tot}^{(-)}(x)$, the method described in section 4 is applied, with $V_{tot}^{(+)}(x)$ and $V_{tot}^{(-)}(x)$ as the target total potentials. It is assumed that the two systems have the same ionized donor density $N_D(x)$, temperature T, permittivity ϵ, and effective electron mass m_e^*. The chemical potentials $\mu^{(+)}$ and $\mu^{(-)}$ are evaluated by the method described in subsection 3.2, and are dependent on the ionized donor density $N_D(x)$, the temperature T, and the eigenvalues $E_n^{(+)}$ and $E_n^{(-)}$. The two-dimensional densities $n_j^{(+)}$ and $n_j^{(-)}$ are then evaluated using equation (16), from which it follows that the total electron densities are

$$n^{(+)}(x) = \sum_j n_j^{(+)} |\psi_j^{(+)}(x)|^2 \tag{22}$$

$$n^{(-)}(x) = \sum_j n_j^{(-)} |\psi_j^{(-)}(x)|^2. \tag{23}$$

Substituting the electron densities $n^{(+)}(x)$ and $n^{(-)}(x)$ and the ionized donor density $N_D(x)$ into equation (11) (the Poisson equation) and solving yields the electric potentials $\Phi^{(+)}$ and $\Phi^{(-)}$ generated by the ionized donors and the conduction band electrons in a system of total potential $V_{tot}^{(+)}(x)$ and $V_{tot}^{(-)}(x)$, respectively. Finally, applying equation (20), it follows that the on-site potentials that produce the total potentials $V_{tot}^{(+)}(x)$ and $V_{tot}^{(-)}(x)$ are

$$V_{os}^{(+)}(x) = V_{tot}^{(+)} + e\Phi^{(+)} \tag{24}$$

$$V_{os}^{(-)}(x) = V_{tot}^{(-)} + e\Phi^{(-)}. \tag{25}$$

Thus, $\psi_n^{(+)}$, $E_n^{(+)}$ and $\psi_n^{(-)}$, $E_n^{(-)}$ are solutions of the self-consistent Schrödinger equation for media with ionized donor concentration $N_D(x)$ and on-site potentials $V_{os}^{(+)}(x)$ and $V_{os}^{(-)}(x)$, respectively. Furthermore, $V_{os}^{(+)}(x)$ and $V_{os}^{(-)}(x)$ generate the total potentials $V_{tot}^{(+)}(x)$ and $V_{tot}^{(-)}(x)$ that were evaluated to be supersymmetric partner potentials. Thus, for the given ionized donor density $N_D(x)$, temperature T, permittivity ϵ, and effective electron mass m_e^*, $V_{os}^{(+)}(x)$ and $V_{os}^{(-)}(x)$ are isospectral on-site potentials, since $E_n^{(+)} = E_n^{(-)}$, except for the case where index $n = 0$.

When evaluating the electrostatic potential Φ, the eigenfunctions ψ_n are used to find the total electron density $n(x)$. In the zero temperature case, only a finite number of eigenstates below the Fermi energy are occupied, and it is possible to include all of them in the calculation. However, for finite temperature, an infinite number of eigenstates have non-zero occupation probability. Due to Fermi–Dirac statistics, sub-band eigenstates with higher eigenenergies have lower electron occupation probability. Thus, in practice, only eigenstates with eigenenergies up to a finite energy are included in the numerical calculation. This introduces error to the total potential V_{tot}, and thus to the final eigenfunctions ψ_n and the operator $\hat{A}$ used to evaluate the partner potentials. The error can be made arbitrarily small by increasing the number of eigenstates included in the calculation.

6. Self-consistent solutions of the rectangular potential well with infinite barrier energy and its partner potential

In this section, basic examples of supersymmetric quantum mechanics and self-consistent solutions of the Schrödinger-Poisson equations are discussed. In doing so, examples of the method discussed in section 5, in which supersymmetric partner *total* potentials are calculated, will be shown.

6.1. The rectangular potential well with infinite barrier energy and its partner potential

Consider single-electron states in a rectangular potential well with infinite barrier energy

$$V(x) = \begin{cases} 0 & 0 < x < L \\ \infty & x \geqslant L,\ x \leqslant 0 \end{cases}, \tag{26}$$

where L is the thickness of the well and defines the domain of interest. Suppose that the well contains *no* ionized donors, and consider a single electron in the conduction band. In this case, the self-consistent model described in section 3 need not be used to solve for the eigenstates and eigenvalues. The method described in section 2 may be used directly to calculate the partner potentials $V^{(-)}(x)$ and $V^{(+)}(x)$.

The ground state of $V(x)$ is $\psi_0 = \sqrt{2/L}\,\sin(\pi x/L)$, and has energy $E_0 = \frac{\pi^2\hbar^2}{2m_e^* L^2}$ (where m_e^* is the effective electron mass), so that

$$V^{(-)}(x) = \begin{cases} -E_0 & 0 < x < L \\ \infty & x \geqslant L,\ x \leqslant 0 \end{cases} \tag{27}$$

and, applying equation (5) and simplifying [17, 18],

$$V^{(+)}(x) = \begin{cases} -E_0 + \dfrac{2E_0}{\sin^2(\pi x/L)} & 0 < x < L \\ \infty & x \geqslant L,\ x \leqslant 0. \end{cases} \tag{28}$$

From equation (8), it follows that

$$\psi_n^{(+)} = \frac{\sqrt{2/L}}{\sqrt{(n+1)^2 - 1}}\left[(n+1)\cos\left(\frac{(n+1)\pi x}{L}\right) - \cot\left(\frac{\pi x}{L}\right)\sin\left(\frac{(n+1)\pi x}{L}\right)\right], \tag{29}$$

where $n = 1, 2, 3, \ldots$ The two lowest-energy eigenstates of $H^{(+)}$ are

$$\psi_1^{(+)} = \sqrt{\frac{8}{3L}}\sin^2\left(\frac{\pi x}{L}\right) \tag{30}$$

and

$$\psi_2^{(+)} = \frac{4}{\sqrt{L}}\cos\left(\frac{\pi x}{L}\right)\sin^2\left(\frac{\pi x}{L}\right). \tag{31}$$

Suppose that the rectangular potential well and its partner potential are made of $Al_xGa_{1-x}As$, where the value of the potential in a given region is controlled by the alloy composition ratio of Al to Ga, and suppose furthermore that there are no ionized donors. In this case, the effective electron mass is $m_e^* = 0.07 \times m_0$, where m_0 is the bare electron mass, and the low-frequency relative permittivity is $\epsilon_{r0} = 13.2$. Figure 1 shows $V^{(-)}(x)$ and $V^{(+)}(x)$ (solid and dashed curves, respectively) for a well of thickness $L = 20$ nm. The ground state energy, E_0, has been added to $V^{(-)}(x)$ and $V^{(+)}(x)$ so that $V^{(-)}(x) = V(x)$. Figure 2 shows the ground state $\psi_0^{(-)}$ and first excited state $\psi_1^{(-)}$ in the presence of $V^{(-)}(x)$, and the ground state $\psi_1^{(+)}$ in the presence of $V^{(+)}(x)$. The greater curvature of the ground state $\psi_1^{(+)}$ gives rise to the higher energy of the state, which is equal to that of the first excited state $\psi_1^{(-)}$.

6.2. Supersymmetry with the rectangular potential well with infinite barrier energy as the *total* potential

Consider now the case where the material contains ionized donors, with uniform ionized donor density $N_D = 5 \times 10^{17}$ cm^{-3} for $0 < x < L$ and electrons maintained at temperature $T = 0$ K, while the rest of the parameters remain the same. Suppose furthermore that we wish the total potentials to be equal to the rectangular potential well with infinite barrier energy and its supersymmetric partner potential, as shown in figure 1, so that $V_{tot}^{(+)} = V^{(+)}$ and $V_{tot}^{(-)} = V^{(-)}$. In this case, the methods described in sections 4 and 5 must be used due to the presence of ionized donors.

The eigenstates ψ_j and eigenvalues E_j of these total potentials can be evaluated by substituting $V_{tot}^{(+)} = V^{(+)}$ and $V_{tot}^{(-)} = V^{(-)}$ into the *non*-self-consistent Schrödinger equation, and will therefore be the

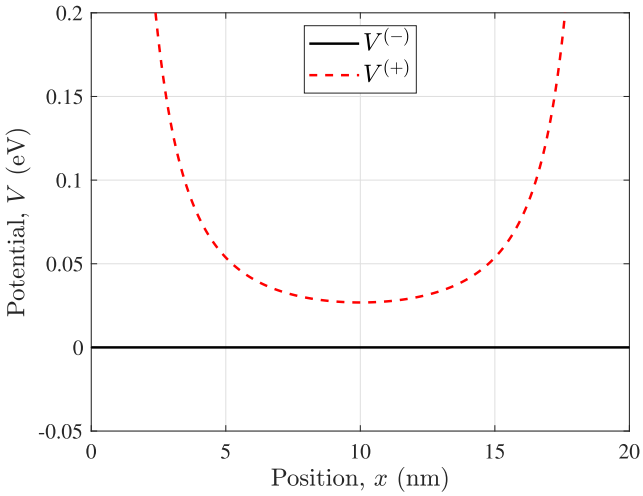

Figure 1. A rectangular potential well with infinite barrier energy $V^{(-)}(x)$ (solid curve) and its partner potential $V^{(+)}(x)$ (dashed curve) as a function of x. Parameters are $m_e^* = 0.07 \times m_0$, $N_D = 0$, and $L = 20$ nm.

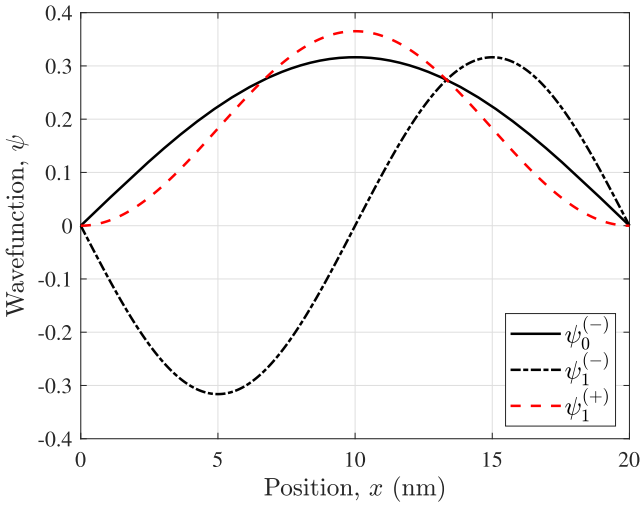

Figure 2. Ground states of the of the rectangular potential well with infinite barrier energy $V^{(-)}(x)$ (solid curve) and its partner potential $V^{(+)}(x)$ (dashed curve) as a function of x. Their eigenenergies are $E_0^{(-)} = 13.4$ meV and $E_1^{(-)} = E_1^{(+)} = 53.7$ meV. Parameters are $m_e^* = 0.07 \times m_0$, $N_D = 0$, and $L = 20$ nm.

same as those shown in figure 2. The electric potentials $\Phi^{(+)}$ and $\Phi^{(-)}$ are evaluated based on the eigenstates, eigenvalues, and system parameters, and the on-site potentials generating the desired total potentials will be

$$V_{os}^{(+)}(x) = V_{tot}^{(+)} + e\Phi^{(+)} \tag{32}$$

$$V_{os}^{(-)}(x) = V_{tot}^{(-)} + e\Phi^{(-)}. \tag{33}$$

Figure 3 shows the on-site potentials $V_{os}^{(-)}(x)$ and $V_{os}^{(+)}(x)$ (solid dashed lines), the target total potentials $V_{target}^{(-)}(x) = V^{(-)}(x)$ and $V_{target}^{(+)}(x) = V^{(+)}(x)$ (thin solid blue lines) and the total potentials numerically evaluated from the on-site potentials $V_{tot}^{(-)}(x)$ and $V_{tot}^{(+)}(x)$ (dashed red lines). The total potentials, when numerically evaluated from the on-site potentials by the self-consistent method described in section 3, converge to the desired target potentials, as can be seen in the figure. Consequently, the eigenstates are the same as those shown in figure 2, and their eigenenergies are also the same.

6.3. Supersymmetry with the rectangular potential well with infinite barrier energy as the *on-site* potential

Suppose that, instead of the total potential V_{tot} being a rectangular potential well with infinite barrier energy, it is the on-site potential V_{os} that is a rectangular potential well with infinite barrier energy. Suppose

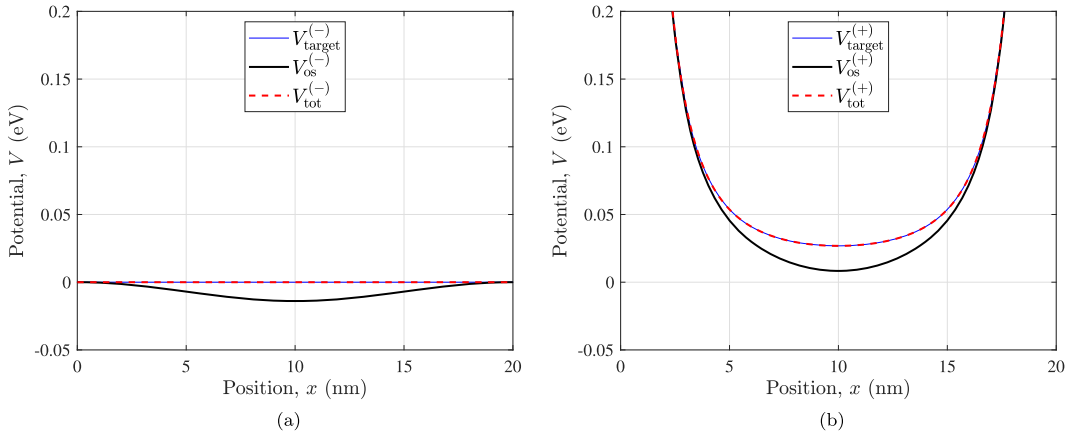

Figure 3. The *total* potential $V_{\text{tot}}^{(-)}(x)$ equal to the infinite rectangular potential well, and the on-site potential $V_{\text{os}}^{(-)}(x)$ that generates it (a), as well as its partner total potential $V_{\text{tot}}^{(+)}(x)$, and the on-site potential $V_{\text{os}}^{(+)}(x)$ that generates it (b). The total potentials $V_{\text{tot}}^{(-)}(x)$ and $V_{\text{tot}}^{(+)}(x)$ are the supersymmetric partner potentials shown in figure 1, and the eigenstates are given in figure 2. Parameters are $m_{\text{e}}^{*} = 0.07 \times m_0$, $N_{\text{D}} = 5 \times 10^{17}$ cm^{-3}, $\epsilon_{\text{r0}} = 13.2$, $T = 0$ K, and $L = 20$ nm.

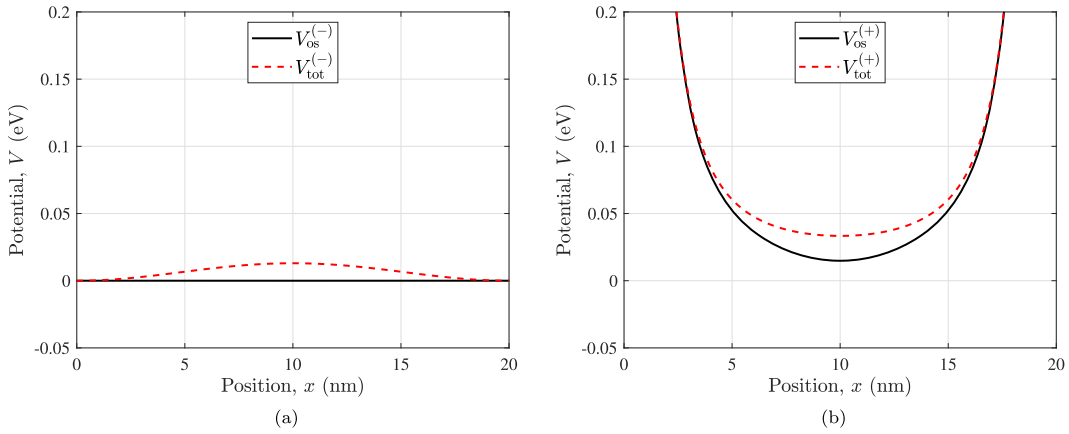

Figure 4. The *on-site* potential $V_{\text{os}}^{(-)}(x)$ equal to the infinite rectangular potential well, and the total potential $V_{\text{tot}}^{(-)}(x)$ that it generates (a), as well as its partner on-site potential $V_{\text{os}}^{(+)}(x)$, and the total potential $V_{\text{tot}}^{(+)}(x)$ that it generates (b). The total potentials $V_{\text{tot}}^{(-)}(x)$ and $V_{\text{tot}}^{(+)}(x)$ are supersymmetric partner potentials. Parameters are $m_{\text{e}}^{*} = 0.07 \times m_0$, $N_{\text{D}} = 5 \times 10^{17}$ cm^{-3}, $\epsilon_{\text{r0}} = 13.2$, $T = 0$ K, and $L = 20$ nm.

furthermore that, as in subsection 6.2, the ionized donor density is $N_{\text{D}} = 5 \times 10^{17}$ cm^{-3}, and the electrons are maintained at temperature $T = 0$ K. In this case, the total potential V_{tot} would not be a rectangular potential well, due to the contribution of the electric potential produced by the ionized donors and conduction band electrons. Nevertheless, using the method described in section 5, it is possible to evaluate supersymmetric partner total potentials $V_{\text{tot}}^{(-)}$ and $V_{\text{tot}}^{(+)}$ using the total potential V_{tot} generated by V_{os}, from which partner on-site potentials $V_{\text{os}}^{(-)}$ and $V_{\text{os}}^{(+)}$ that generate these total potentials can be evaluated. Notably, because $V_{\text{tot}}^{(-)} = V_{\text{tot}} - E_0$, it follows that $V_{\text{os}}^{(-)} = V_{\text{os}} - E_0$, so that $V_{\text{os}}^{(-)}$ will be a rectangular potential well with infinite barrier energy.

Figure 4 shows the partner on-site potentials $V_{\text{os}}^{(-)}$ and $V_{\text{os}}^{(+)}$ (solid black curves) and the supersymmetric partner total potentials $V_{\text{tot}}^{(-)}$ and $V_{\text{tot}}^{(+)}$ (dashed red curves) evaluated from the on-site potential $V_{\text{os}}(x) = V(x)$, where $V(x)$ is the rectangular potential well with infinite barrier energy defined in equation (26), with thickness $L = 20$ nm. Note the bulge in the total potentials near the center of the well, where the electron density is greatest.

6.4. Partner on-site potentials are a function of ionized donor density

While it is possible to speak of 'partner on-site potentials' due to the fact that they generate supersymmetric partner total potentials, it is important to note that this is only possible if other system parameters have the required values. The effective electron mass, the permittivity, and, notably, the temperature and the ionized donor density, must all have the particular values used to evaluate the partner on-site potentials in order to

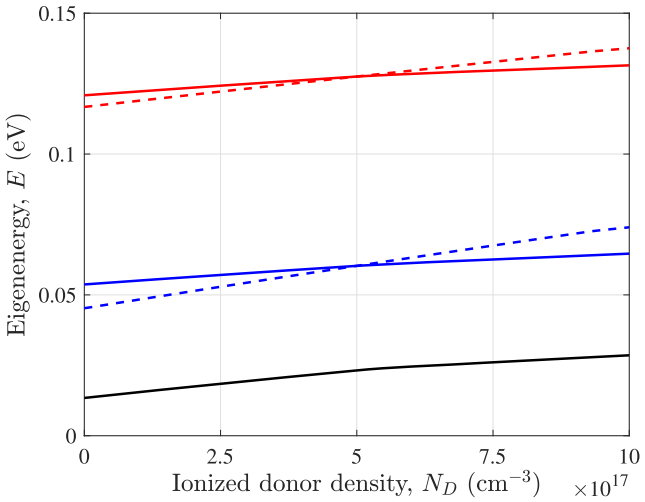

Figure 5. Eigenenergies calculated as a function of ionized donor density N_D in a rectangular potential well with infinite barrier energy $V_{os}^{(-)}$ (solid curves) and its partner on-site potential $V_{os}^{(+)}$ (dashed curves) using the Schrödinger and Poisson equations. The on-site potentials are those shown in figure 4, and are isospectral if $N_D = 5 \times 10^{17}$ cm^{-3}. Parameters are $m_e^* = 0.07 \times m_0$, $\epsilon_{r0} = 13.2$, $T = 0$ K, $L = 20$ nm.

yield supersymmetric partner total potentials. If these parameters differ from the required values, then isospectrality will be broken.

Consider two systems with the on-site potentials $V_{os}^{(+)}$ and $V_{os}^{(-)}$ evaluated in subsection 6.3, as shown in figure 4, with equal but unknown constant ionized donor density N_D, and otherwise with the same system parameters assumed in subsection 6.3 (effective mass $m_e^* = 0.07 \times m_0$, relative permittivity $\epsilon_{r0} = 13.2$, temperature $T = 0$ K, and total thickness $L = 20$ nm). Let $\hat{H}^{(+)}$ and $\hat{H}^{(-)}$ be the Hamiltonians of an electron in the systems with on-site potentials $V_{os}^{(+)}$ and $V_{os}^{(-)}$, respectively. If $N_D = 5 \times 10^{17}$ cm^{-3}, then the systems will be identical to those discussed in subsection 6.3, and $\hat{H}^{(+)}$ and $\hat{H}^{(-)}$ will be isospectral when solved self-consistently, except for the ground state of $\hat{H}^{(-)}$, which has no counterpart. On the other hand, if $N_D \ll 5 \times 10^{17}$ cm^{-3} or $N_D \gg 5 \times 10^{17}$ cm^{-3}, then upon solving the Schrödinger-Poisson equations, the total potentials will differ substantially from those shown in figure 4, and consequently the eigenstates and eigenenergies will also differ significantly.

Figure 5 shows the eigenenergies $E_j^{(+)}$ of $\hat{H}^{(+)}$ (dashed curves) and $E_j^{(-)}$ of $\hat{H}^{(-)}$ (solid curves) as a function of the ionized donor density N_D. As expected, the eigenenergies are equal only at $N_D = 5 \times 10^{17}$ cm^{-3}. The eigenenergies increase as a function of ionized donor density N_D. This is because the presence of more electrons in the conduction band increases the potential near the center of the well. This effect is reduced at higher temperatures because occupation of higher energy states in the conduction band causes more uniform electron distribution and hence a less pronounced increase in potential near the center of the well.

Because the eigenfunctions of $\hat{H}^{(+)}$ differ from the eigenfunctions of $\hat{H}^{(-)}$, the impact of the self-consistent solution on the eigenvalues also differs. In particular, the eigenfunctions of $\hat{H}^{(+)}$ are more localized near the center of the well, meaning that they experience a larger electric potential near the center of the well in comparison to that experienced by the eigenfunctions of $\hat{H}^{(-)}$. Once again, the magnitude of this effect is reduced at higher temperatures. The sensitivity to separation of the eigenergies of $\hat{H}^{(+)}$ and $\hat{H}^{(-)}$ with increasing ionized donor density N_D can be enhanced by increasing L.

7. Distinguishing partner potentials

In the following, supersymmetric partner total potentials are evaluated in the presence of ionized donors using the method discussed in section 5. Time-independent partner potentials have Hamiltonians that are isospectral (with the possible exception of the ground state). However, their eigenfunctions are not identical in the general case. The question arises as to whether it is possible to distinguish partner potentials without having to resort to the direct measurement of potentials.

One way to do so is to subject the potentials to a perturbation (such as an applied electric field) which breaks symmetry and introduces a shift in energy eigenvalues. If this shift differs between one partner potential and the other, the energy eigenvalues will no longer be identical. This provides a measure by which to spectrally distinguish between systems.

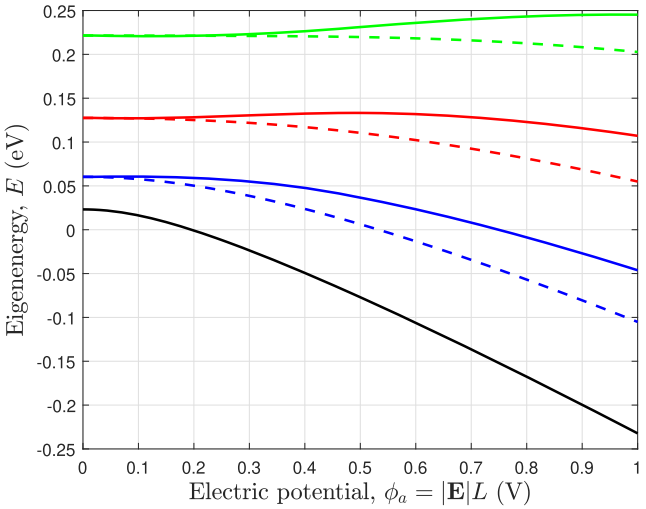

Figure 6. Eigenenergies as a function of $\phi_a = |\mathbf{E}|L$ in a rectangular potential well with infinite barrier energy. Parameters are $m_e^* = 0.07 \times m_0$, $N_D = 5 \times 10^{17}$ cm^{-3}, $\epsilon_{r0} = 13.2$, $T = 0$ K, and $L = 20$ nm.

7.1. A rectangular potential well with infinite barrier energy

As a first example, consider a rectangular potential well with infinite barrier energy containing ionized donors, with onsite potential V_{os} given by equation (26). Let $V_{os}^{(-,0)}$ and $V_{os}^{(+,0)}$ be the corresponding unperturbed onsite potentials calculated using the self-consistent method described in section 5 to account for the effect of the presence of ionized donors, so that the corresponding total potentials $V_{tot}^{(-,0)}$ and $V_{tot}^{(+,0)}$ are supersymmetric partner potentials. Suppose that the potential well and its partner potential are perturbed by an applied voltage ϕ_a that is zero-centered, so that the voltage applied on the left of the well is $+\phi_a/2$ and the voltage applied on the right is $-\phi_a/2$. Such a bias voltage generates a constant electric field $\mathbf{E}$ in the x direction, so that $|\mathbf{E}| = \frac{\phi_a}{L}$, and the onsite potentials become

$$V_{os}^{(-)} = V_{os}^{(-,0)} + \delta V(x) \tag{34}$$

$$V_{os}^{(+)} = V_{os}^{(+,0)} + \delta V(x), \tag{35}$$

where

$$\delta V(x) = e|\mathbf{E}|(x - L/2). \tag{36}$$

Suppose that the ionized donor density is $N_D = 5 \times 10^{17}$ cm^{-3}. Figure 6 shows the energy eigenvalues of $\hat{H}^{(-)}$ and $\hat{H}^{(+)}$ as a function of $\phi_a = |\mathbf{E}|L$ for the case where $L = 20$ nm. As ϕ_a increases, the eigenvalues of $\hat{H}^{(-)}$ and $\hat{H}^{(+)}$, which are identical when $\phi_a = 0$, gradually diverge.

7.2. Potential step in a potential well with infinite barrier energy

Suppose a potential step is added to the rectangular well with infinite barrier energy, so that the unperturbed on-site potential becomes

$$V_{os}(x) = \begin{cases} V_{step} & 0 < x < w_{step} \\ 0 & w_{step} < x < L, \\ \infty & x \geqslant L,\ x \leqslant 0 \end{cases} \tag{37}$$

where w_{step} is the thickness of the potential step and V_{step} is the potential energy of the step. Suppose furthermore that the step and well are made of $Al_xGa_{1-x}As$, so that $m_e^* = 0.07 \times m_0$ and $\epsilon_r = 13.2$. Let the carrier density be $N_D = 5 \times 10^{17}$ cm^{-3}, and let $V_{os}^{(-,0)}(x)$ and $V_{os}^{(+,0)}(x)$ be the partner potentials calculated from $V_{os}(x)$ by the method described in section 5.

If $V_{os}^{(-,0)}$ and $V_{os}^{(+,0)}$ are perturbed by an applied voltage ϕ_a that is zero-centered, so that the voltage applied on the left of the well is $+\phi_a/2$ and the voltage applied on the right is $-\phi_a/2$, then such a bias voltage generates a constant electric field $\mathbf{E}$ in the x direction, so that $|\mathbf{E}| = \phi_a/L$, and the potentials are given by equations (34) and (35), where $\delta V(x)$ is given by equation (36).

Figure 7 shows the eigenvalues of $\hat{H}^{(-)}$ and $\hat{H}^{(+)}$ as a function of $\phi_a = |\mathbf{E}|L$ for the case where $L = 20$ nm. In the domain, the thickness of the potential step is $w_{step} = 15.2$ nm and the step energy is $V_{step} = 0.35$ eV.

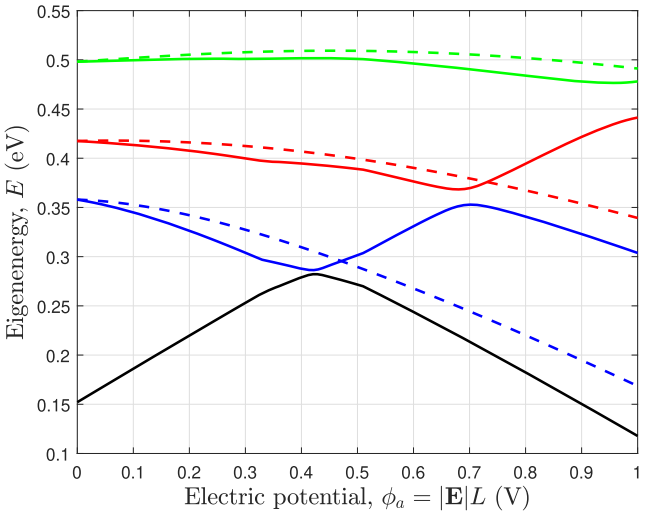

Figure 7. Eigenenergies as a function of $\phi_a = |\mathbf{E}|L$ for a rectangular well with infinite barrier energy containing a potential step (solid curves) and for its partner potential (dashed curves). The rectangular well has thickness $L = 20$ nm, and contains a potential step of thickness $w_{\text{step}} = 15.2$ nm and potential $V_{\text{step}} = 0.35$ eV. Other parameters are $m_e^* = 0.07 \times m_0$, $N_D = 5 \times 10^{17}$ cm^{-3}, $\epsilon_{r0} = 13.2$, and temperature $T = 0$ K.

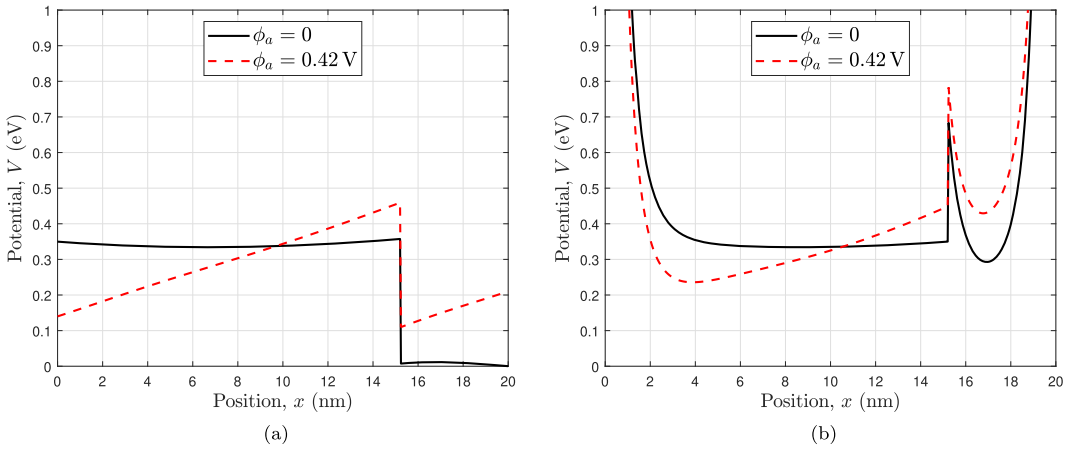

Figure 8. Potentials (a) $V_{\text{tot}}^{(-)}$ and (b) $V_{\text{tot}}^{(+)}$ as a function of position x for $\phi_a = |\mathbf{E}|L = 0$ (solid curve) and $\phi_a = |\mathbf{E}|L = 0.42$ V (dashed curve). Parameters are: domain thickness $L = 20$ nm, $m_e^* = 0.07 \times m_0$, $N_D = 5 \times 10^{17}$ cm^{-3}, $\epsilon_{r0} = 13.2$, $T = 0$ K, $w_{\text{step}} = 15.2$ nm, and $V_{\text{step}} = 0.35$ eV.

For these particular dimensions of the well and the potential step, the eigenenergy of the ground state of $\hat{H}^{(-)}$ is less than the potential of the barrier, meaning that, in the absence of a perturbation, it is bound in the well created by the potential step. When the system is perturbed by an external electric field, the energy of the ground state initially increases, as the potential of the floor of the finite well rises with respect to the rest of the potential. Eventually, with increasing externally applied electric field, the ground state becomes no longer localized near the well. The peak in electron density then switches to the other side of the domain. The total potentials $V_{\text{tot}}^{(-)}$ and $V_{\text{tot}}^{(+)}$, without perturbation, and with perturbation at the switching point, are shown in figure 8. The wave functions near this switching point are shown in figure 9.

Note that, as a function of ϕ_a, the difference between $E_0^{(-)}$ and $E_1^{(-)}$ decreases until reaching a minimum at the switching point ($\phi_a = 0.42$ V), then begins to increase. Meanwhile, $E_1^{(+)}$ continues to decrease as a function of ϕ_a because of the absence of a $\psi_0^{(+)}$ state. The result is a crossing point between $E_1^{(-)}$ and $E_1^{(+)}$ at which these eigenvalues diverge more quickly as a function of ϕ_a than they do in the case of the rectangular potential well with infinite barrier energy (compare figures 6 and 7).

For a given pair of supersymmetric partner potentials, symmetry can also be broken by a change of temperature. The sensitivity to this symmetry breaking with increasing temperature can be enhanced by increasing L. Figure 10 shows eigenenergies calculated self-consistently as a function of temperature in a rectangular well containing a potential step (solid curves) and its partner potential (dashed curves).

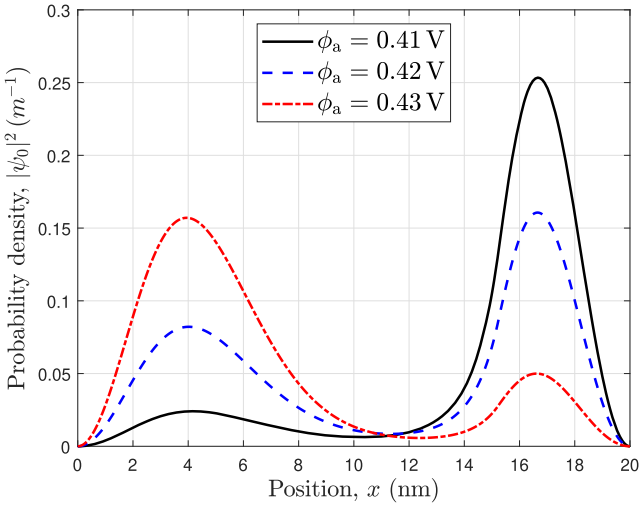

Figure 9. Probability distributions $|\psi_0^{(-)}(x)|^2$ as a function of position x in the vicinity of the switching point at which the perturbing electric field causes the wave function to move from the right to the left of the domain $(0 < x < L)$. Parameters are $m_e^* = 0.07 \times m_0$, $N_D = 5 \times 10^{17}$ cm^{-3}, $\epsilon_{r0} = 13.2$, $T = 0$ K, $L = 20$ nm, $w_{step} = 15.2$ nm, and $V_{step} = 0.35$ eV.

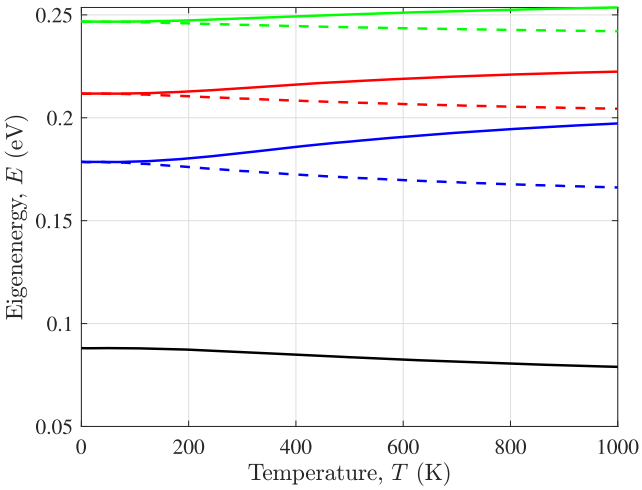

Figure 10. Eigenenergies as a function of temperature in a rectangular well with infinite barrier energy containing a potential step (solid curves) and its partner potential (dashed curves). The partner potentials are calculated using the method described in section 5 (taking into account self-consistency) at $T = 0$ K. Parameters are $m_e^* = 0.07 \times m_0$, $\epsilon_{r0} = 13.2$, and $N_D = 5 \times 10^{17}$ cm^{-3}, $L = 30$ nm, $w_{step} = 22.8$ nm, $V_{step} = 0.2$ eV, and $\phi_a = 0$.

7.3. Maximizing the rate of separation of supersymmetric partners

Given two supersymmetric Hamiltonians $\hat{H}^{(+)}$ and $\hat{H}^{(-)}$ as defined in section 2, the ground state of $\hat{H}^{(+)}$ will have the same eigenenergy as the first excited state of $\hat{H}^{(-)}$. Subsections 7.1 and 7.2 show how a perturbation may be used to distinguish the partner potentials by exploiting the fact that the eigenfunctions corresponding to the isospectral states are not identical. For small perturbations, the rate of separation is slow. However, once the perturbations are large enough to cause the wave functions to switch from one side of the domain to the other, rapid increases in the difference in eigenenergies between formerly isospectral states can occur.

This spatial switching of the wave functions leads to the change in slope observed in figure 7. The change in slope leads to the crossing of the curves corresponding to the eigenvalues of the ground state of $\hat{H}^{(+)}$ and the first excited state of $\hat{H}^{(-)}$. It is near this point of crossing that $E_1^{(+)}$ and $E_1^{(-)}$ diverge most rapidly. The question then arises as to whether the parameters of the potential step may be adjusted to maximize this rate of separation.

Figure 11 shows the rate of change of the difference between the eigenenergy of the ground state of $\hat{H}^{(+)}$ and the first excited state of $\hat{H}^{(-)}$ with respect to the bias voltage $(\frac{d(\Delta E_{1,1}^{(-,+)})}{d\phi_a} = \frac{d(E_1^{(-)} - E_1^{(+)})}{d\phi_a})$ plotted as a function of step thickness w_{step} and the potential of the step V_{step}. The effective electron mass is

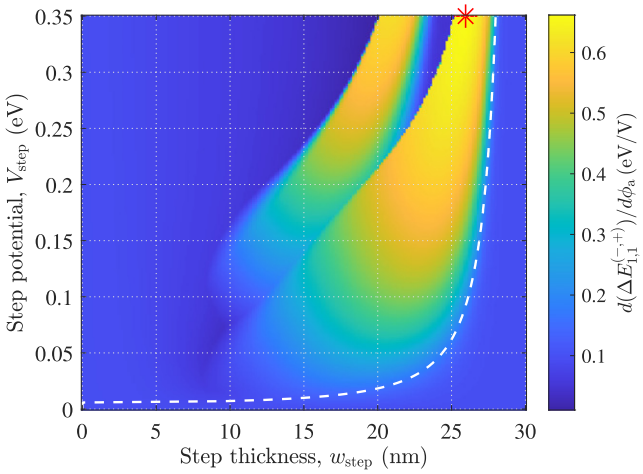

Figure 11. The maximum rate of change of the difference between $E_1^{(+)}$ and $E_1^{(-)}$ with respect to the bias voltage ($\frac{\mathrm{d}(E_1^{(-)}-E_1^{(+)})}{\mathrm{d}\phi_a}$) plotted as a function of step thickness w_{step} and the potential energy of the step V_{step}. The bias voltage $\phi_a = |\mathbf{E}|L$ ranges from 0 to 0.35 V. The point where the maximum slope is achieved is indicated by the asterisk, and corresponds to $V_{\text{step}} = 0.35$ eV and $w_{\text{step}} = 25.95$ nm. Other parameters are $m_e^* = 0.07 \times m_0$, $N_D = 0$, $\epsilon_{r0} = 13.2$, $T = 0$ K, and $L = 30$ nm. Below the dashed line, no bound states exist in the potential well created by the potential step.

$m_e^* = 0.07 \times m_0$ and domain thickness $L = 30$ nm. The point where the maximum slope of 0.662 eV V^{-1} is achieved is indicated by the asterisk, and corresponds to $V_{\text{step}} = 0.35$ eV and $w_{\text{step}} = 25.95$ nm. To generate this plot, the potential energy drop across the domain caused by the applied electric field is varied from 0 eV to 0.35 eV. The maximum of the derivative $\frac{\mathrm{d}(\Delta E_{1,1}^{(-,+)})}{\mathrm{d}V_{\text{field}}}$ is then evaluated.

When the energy of an eigenstate is equal to the potential of the step, eigenfunctions of $\hat{H}^{(-)}$ have the form

$$\psi^{(-)}(x) = \begin{cases} Ax & 0 < x < w_{\text{step}} \\ B\,\sin\left[k(x-L)\right] & w_{\text{step}} < x < L, \end{cases} \tag{38}$$

from which it follows, after applying the boundary conditions at $x = w_{\text{step}}$, that $A = Bk\,\cos\left[k(w_{\text{step}} - L)\right]$, where B is then a normalization constant, and

$$kw_{\text{step}} = \tan\left[k(w_{\text{step}} - L)\right]. \tag{39}$$

The white dashed curve in figure 11 indicates the values of w_{step} and L for which a solution for k in equation (39) exists and is the ground state of the system. Thus, for the region below the dashed curve, no states exist that are bound within the well created by the potential step, while for the region above the dashed curve, such a state always exists. The lack of any states bound in the potential well of thickness $L - w_{\text{step}}$ in the region below the dashed curve explains the low maximum rates of separation in that region.

It can be seen in figure 11 that the slope increases with increasing step potential V_{step}. The slope is maximized when the potential step occupies most of the well, leaving a relatively narrow well of thickness $L - w_{\text{step}}$ within the domain of thickness L. The secondary region with high rates of separation seen in figure 11 is caused by the first excited state also being bound in the well created by the potential step. While the maximum bias voltage of 0.35 V is not sufficient to cause the expectation value of position of the ground state to shift to the other side of the domain in this region, it is sufficient to cause the first excited state to shift due to its higher energy.

8. Distinguishing strictly isospectral potentials

One possible objection to the results presented in section 7 is that the partner Hamiltonians are not strictly isospectral, since there is no eigenstate of $\hat{H}^{(+)}$ with the same eigenenergy as the ground state of $\hat{H}^{(-)}$. It therefore remains to be shown that the substantially different behavior of the partner systems when subject to perturbation is not merely a consequence of the absence of a $\psi_0^{(+)}$ state. One way of demonstrating this is to show that similar behavior can be observed for self-consistent solutions to the Schrödinger-Poisson equations in strictly isospectral potentials when they are subject to perturbation.

The ability to distinguish strictly isospectral potentials by perturbation relies partly on the fact that subjecting the potentials to the same perturbation will affect the localization of the wavefunctions in each

potential differently. While previous research has explored how the localization of wavefunctions in strictly isospectral potentials is affected by the parameters of the potentials [19], which do not affect isospectrality, in this case the change in localization is due to perturbation, which breaks isospectrality.

8.1. Strictly isospectral potentials

For any potential $V(x)$ with N bound eigenstates, there is an N-parameter family of strictly isospectral potentials $V(\lambda_1, \lambda_2, \ldots, \lambda_N; x)$ with the same eigenenergies as $V(x)$, where $\lambda_1, \lambda_2, \ldots, \lambda_N$ are real numbers [3, 5]. In the simplest case, any potential with one or more bound states has a one-parameter family of isospectral potentials $V(\lambda; x)$ [4]. In the following, only this one-parameter case is studied.

Consider a potential $V(x)$ with ground state ψ_0, ground state energy E_0, and partner potentials $V^{(-)}(x)$ and $V^{(+)}(x)$ calculated from $V(x)$ as shown in section 2, so that

$$V^{(-)}(x) = W^2(x) - \frac{\hbar}{\sqrt{2m}} W'(x) \tag{40}$$

$$V^{(+)}(x) = W^2(x) + \frac{\hbar}{\sqrt{2m}} W'(x), \tag{41}$$

where $W(x) = -\frac{\hbar}{\sqrt{2m_0}} \frac{\psi_0'}{\psi_0}$. Let $\tilde{W}(x)$ by any superpotential that satisfies the equation $V^{(+)}(x) = \tilde{W}^2(x) + \frac{\hbar}{\sqrt{2m}} \tilde{W}'(x)$, and let $\frac{1}{y(x)} = \tilde{W} - W$. It follows that

$$V^{(+)}(x) = W^2(x) + \frac{\hbar}{\sqrt{2m}} W'(x) \tag{42}$$

$$= \tilde{W}^2(x) + \frac{\hbar}{\sqrt{2m}} \tilde{W}'(x) \tag{43}$$

$$= \left(W + \frac{1}{y}\right)^2 + \frac{\hbar}{\sqrt{2m}} \frac{\mathrm{d}}{\mathrm{d}x} \left(W + \frac{1}{y}\right), \tag{44}$$

which, upon simplification, is the differential equation

$$y' = \frac{\sqrt{2m}}{\hbar} \left(2Wy + 1\right). \tag{45}$$

Solving this equation yields

$$y = \frac{\sqrt{2m_0}}{\hbar} \frac{1}{\psi_0^2} \left[\int_0^x \psi_0^2(x')\mathrm{d}x' + \lambda\right]. \tag{46}$$

It follows that

$$\tilde{W}(\lambda; x) = W + \frac{1}{y} = \frac{\hbar}{\sqrt{2m_0}} \left[\frac{\psi_0^2}{I(x) + \lambda} - \frac{\psi_0'}{\psi_0}\right], \tag{47}$$

where $I(x) = \int_0^x \psi_0^2(x')\mathrm{d}x'$. The potential

$$\tilde{V}^{(-)}(x) = \tilde{W}^2(x) - \frac{\hbar}{\sqrt{2m}} \tilde{W}'(x) \tag{48}$$

is then a supersymmetric partner of $V^{(+)}(x)$, implying that $V^{(+)}(x)$ and $\tilde{V}^{(-)}(x)$ are isospectral except for the ground state energy $\tilde{E}_0^{(-)}$. Substituting $\tilde{W} = -\frac{\hbar}{\sqrt{2m}} \frac{\tilde{\psi}_0'}{\tilde{\psi}_0}$ and $W(x) = -\frac{\hbar}{\sqrt{2m_0}} \frac{\psi_0'}{\psi_0}$ into equation (47), it follows that the ground state of $\tilde{V}^{(-)}(x)$ is [4]

$$\tilde{\psi}_0(\lambda; x) = \frac{A\psi_0}{I(x) + \lambda}, \tag{49}$$

where A is the normalization constant. Furthermore, its eigenenergy is $\tilde{E}_0^{(-)} = E_0^{(-)} = 0$. Therefore, $\tilde{V}^{(-)}(x)$ and $V^{(-)}(x)$ are strictly isospectral (i.e. they share all eigenvalues).

A method analogous to that described in section 5 may be used to calculate strictly isospectral potentials when solving the Schrödinger-Poisson equations self-consistently.

8.2. Perturbing strictly isospectral potentials

Figure 12 shows the total potential $V_{\mathrm{tot}}^{(-)}(x)$ for a rectangular potential well of thickness $L = 20$ nm with infinite barrier energy containing a potential step of thickness $w_{\mathrm{step}} = 15.2$ nm and potential energy $V_{\mathrm{step}} = 0.35$ eV (solid curves), together with the strictly isospectral potentials (dashed curves)

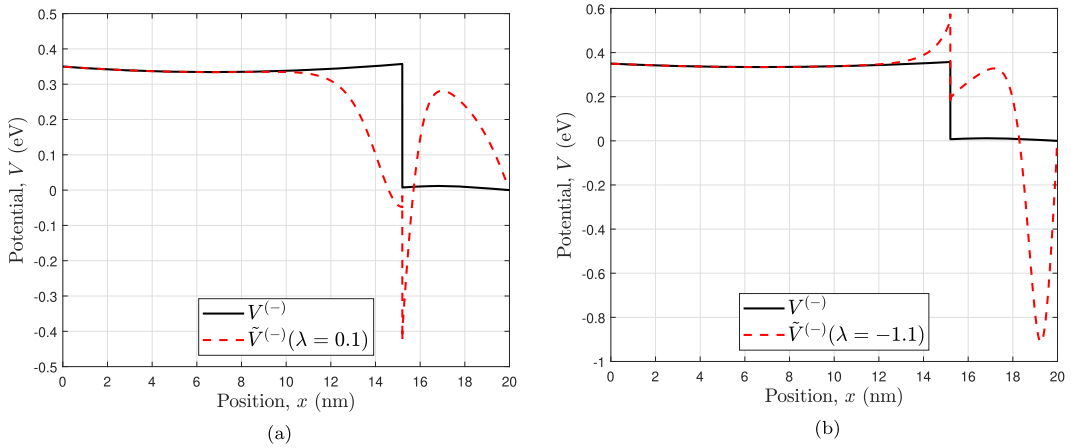

Figure 12. The total potential of a rectangular potential well with infinite barrier energy containing a potential step $V_{\text{tot}}^{(-)}(x)$ (solid curve) and for a member of the family of one parameter potentials strictly isospectral to it (dashed curves) with (a) parameter $\lambda = 0.1$ and (b) $\lambda = -1.1$. The rectangular well has thickness $L = 20$ nm, and contains a potential step of thickness $w_{\text{step}} = 15.2$ nm and potential energy $V_{\text{step}} = 0.35$ eV. Other parameters are $m_{\text{e}}^* = 0.07 \times m_0$, $N_{\text{D}} = 5 \times 10^{17}$ cm^{-3}, $\epsilon_{\text{r0}} = 13.2$, and $T = 0$ K.

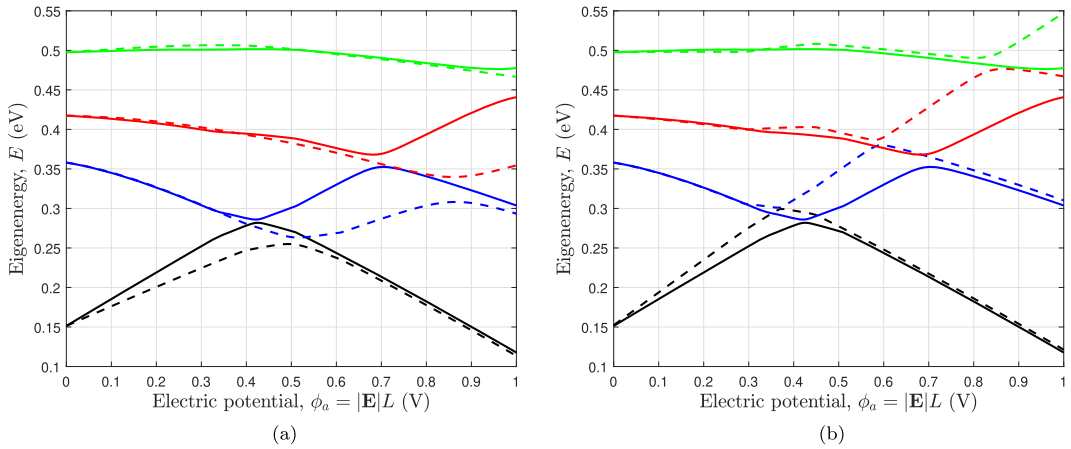

Figure 13. Eigenenergies as a function of $\phi_{\text{a}} = |\mathbf{E}|L$ for a rectangular well with infinite barrier energy containing a potential step (solid curves) and for a member of the family of one parameter potentials strictly isospectral to it (dashed curves) with (a) parameter $\lambda = 0.1$ and (b) $\lambda = -1.1$. The rectangular well has thickness $L = 20$ nm, and contains a potential step of thickness $w_{\text{step}} = 15.2$ nm and potential $V_{\text{step}} = 0.35$ eV. Other parameters are $m_{\text{e}}^* = 0.07 \times m_0$, $N_{\text{D}} = 5 \times 10^{17}$ cm^{-3}, $\epsilon_{\text{r0}} = 13.2$, and $T = 0$ K.

$\tilde{V}_{\text{tot}}^{(-)}(\lambda = 0.1; x)$ and $\tilde{V}_{\text{tot}}^{(-)}(\lambda = -1.1; x)$. As in 7.2, the step and well are made of $Al_xGa_{1-x}As$, so that $m_{\text{e}}^* = 0.07 \times m_0$ and $\epsilon_{\text{r}} = 13.2$, and the carrier density is $N_{\text{D}} = 5 \times 10^{17}$ cm^{-3}.

Figure 13 shows the eigenenergies of these potentials when perturbed by an applied voltage $\phi_{\text{a}} = |\mathbf{E}|L$, where ϕ_{a} is zero-centered, as described in 7.2. Figure 13(a) shows the eigenenergies for $V^{(-)}(x)$ (solid lines) and $\tilde{V}^{(-)}(\lambda = 0.1; x)$ (dashed lines) while figure 13(a) shows the eigenenergies for $V^{(-)}(x)$ and $\tilde{V}^{(-)}(\lambda = -1.1; x)$. Similar to the results shown in figure 7, the energies of the first excited states of $V^{(-)}(x)$ and $\tilde{V}^{(-)}$ separate most quickly after the ground state wave function of $V^{(-)}(x)$ (figure 13(a)) or $\tilde{V}^{(-)}(\lambda)$ (figure 13(b)) shifts from being localized on the right side of the well to being localized on the left side of the well due to no longer being confined in the potential well created by the potential step. Because the ground state wave function shifts in one potential before the other, an energy gap appears between the first excited states of the two potentials.

Note that the first excited states in figure 13 remain nearly isospectral until the switching point is reached. This contrasts with the gradual separation seen in figure 7 for the supersymmetric partner potentials. Unlike in the case of supersymmetric partner potentials, the ground states of strictly isospectral potentials have the same eigenenergy. Furthermore, for the potentials shown in figure 12, only the ground states are bound in the potential well created by the step potential. Orthogonality between the ground-state and excited-states forces the spatial distribution of both first excited-state probabilities to occur in the

potential step region. Since the potentials are similar in this region, the wave functions are also similar, and are thus similarly affected by small perturbations. In this way it is possible to *minimize* sensitivity to excited-state energy eigenvalue separation in the presence of a perturbation.

9. Discussion

The results presented show the existence of self-consistent solutions to the Schrödinger and Poisson equations for isospectral Hamiltonians that include many identical non-interacting electrons. For a given set of parameters there is a total potential that is *static* so that $V_{\rm tot} = V_{\rm tot}(x)$ and it is possible to find the corresponding isopectral partner on-site potentials using the technique described in section 5.

Our study restricted description of electrons to *bound states* with motion in one dimension. Models that include electron motion in three dimensions have not been explored and it remains unknown if supersymmetry concepts can be applied to such cases. Prior research has shown that the absolute values of the transmission (and reflection) coefficients of supersymmetric partner optical dielectric structures are equal [20]. Such matching is also a feature of isospectral electronic systems [4], but it is not known how this extends to scattering in electronic systems modeled by self-consistent Schrödinger-Poisson equations.

Breaking of supersymmetry has been demonstrated by using control parameters such as perturbation via an externally applied electric field, change in temperature, or change in electron charge density. The sensitivity of parameter values used to break supersymmetry and distinguish between initially isospectral systems can be controlled by design of on-site potential profiles. This is possible because of the interplay between self-consistent solutions of the Schrödinger and Poisson equations for a given design of on-site potential profile and the other control parameters of the system.

Insensitivity to energy eigenvalue separation of excited states in the presence of a perturbation can be achieved in strictly isospectral systems in which the Schrödinger and Poisson equations are calculated self-consistently. This robustness to perturbation is obtained by exploiting orthogonality between ground and excited states in the strictly isospectral system.

10. Conclusion

Isospectral Hamiltonians and partner potentials can be found for self-consistent solutions of the Schrödinger and Poisson equations in systems that include identical non-interacting electrons. Our study of isospectral bound electron-states in semiconductor quantum wells shows that perturbation by an external electric field can be used to break symmetry and spectrally distinguish between systems. For a given pair of partner potentials, symmetry may also be broken by a change of electron density or temperature. Device structures can be designed to *maximize* sensitivity to separation of isospectral states between partner states. By exploiting orthogonality between ground and excited states in a strictly isospectral system it is also possible to *minimize* sensitivity to energy eigenvalue separation in the presence of a perturbation.

Data availability statement

The data that support the findings of this study are available upon reasonable request from the authors.

ORCID iDs

Amine Abouzaid https://orcid.org/0000-0002-9499-6894

References

[1] Witten E 1981 *Nucl. Phys.* B **188** 513
[2] Nicolai H 1976 *J. Phys. A: Math. Gen.* **9** 1497
[3] Cooper F, Khare A and Sukhatme U 1995 *Phys. Rep.* **251** 267
[4] Khare A and Sukhatme U 1989 *J. Phys. A: Math. Gen.* **22** 2847
[5] Keung W-Y, Sukhatme U P, Wang Q and Imbo T D 1989 *J. Phys. A: Math. Gen.* **22** L987
[6] Fernandez C D J and Roy B 2020 *Phys. Scr.* **95** 055210
[7] Concha Y, Huet A, Raya A and Valenzuela D 2018 *Mater. Res. Express* **5** 065607
[8] Midya B, Zhao H, Qiao X, Miao P, Walasik W, Zhang Z, Litchinitser N M and Feng L 2019 *Photon. Res.* **7** 363
[9] Hokmabadi M P, Nye N S, El-Ganainy R, Christodoulides D N and Khajavikhan M 2019 *Science* **363** 623
[10] Kac M 1966 *Am. Math. Mon.* **73** 1
[11] Plastino A R, Rigo A, Casas M, Garcias F and Plastino A 1999 *Phys. Rev.* A **60** 4318

[12] Bagchi B, Ganguly A and Sinha A 2010 *Phys. Lett.* A **374** 2397
[13] Bennett A J and Duke C B 1967 *Phys. Rev.* **160** 541
[14] Stern F and Howard W E 1967 *Phys. Rev.* **163** 816
[15] Berkowitz H L and Lux R A 1987 *J. Vac. Sci. Technol.* B **5** 967
[16] Brounkov P N, Benyattou T and Guillot G 1996 *J. Appl. Phys.* **80** 864
[17] Dutt R, Khare A and Sukhatme U P 1988 *Am. J. Phys.* **56** 163
[18] Gutierrez K, León E, Belloni M and Robinett R W 2018 *Eur. J. Phys.* **39** 065404
[19] Rosu H C, Mancas S C and Chen P 2014 *Ann. Phys., NY* **349** 33
[20] Miri M-A, Heinrich M and Christodoulides D N 2014 *Optica* **1** 89